Paper

Improving the GPR Detectability Using a Novel Loop Bowtie Antenna

K. K. Ajith[1,2] and Amitabha Bhattacharya[1]

[1] *Department of Electronics & Electrical Comm. Eng., Indian Institute of Technology Kharagpur, India*
[2] *Department of ETC, International Institute of Information Technology Bhubaneswar, India*

https://doi.org/10.26636/jtit.2017.120917

Abstract—The Ground Penetrating Radar (GPR) technique finds immense applications in civil engineering today, as the most suitable approach for non-destructive testing of pavements, highways, concrete structures, and more. The major challenge in carrying out a GPR evaluation is that the properties of the probed medium are usually unknown. The permittivity and conductivity of the medium may vary from those of air to water. The electromagnetic waves also have a frequency dependent attenuation. The ability of GPR to detect signals reflected and scattered by the targets largely depends upon the antenna performance. This paper studies a novel 11:1 wideband loop bowtie antenna with very good radiation properties in the entire operating bandwidth. Synthetic and experimental results are presented for the return loss and gain of the antenna. Furthermore, experimental results are presented for the radiation patterns in the E- and H-plane. We also used the antenna to measure B-scans over two different pipes, a bamboo, and a reinforced concrete structure. All results obtained with the proposed antenna have been compared with results obtained by using a RC loaded antenna. It has been found that the loop bowtie antenna has excellent detection capability and produces less clutter. The loop loading technique can be applied to existing antennas for improved GPR imaging. This will improve the detectability of GPR by improving the target return signal.

Keywords—antenna, Ground Penetrating Radar, imaging, UHF, UWB.

1. Introduction

Ground Penetrating Radar (GPR) is used in civil engineering for non-destructive testing (NDT) of pavements, roads, bridges, tunnels, and more [1]. It can also be used for rebar detection in concrete [2]. More recent and advanced applications include detecting corrosion of rebar due to contamination by water and salt [3]. Moreover, GPR is a powerful technique in archeological surveys for mapping buried artifacts [4]. In the defense sector, GPR is extensively used for landmine detection [5]. The main objective of GPR is to image subsurface targets or layers for a qualitative analysis. The produced data can also be used for a quantitative study of electromagnetic properties of the medium and targets.

The depth at which a GPR can probe, depends upon the electromagnetic properties of the soil. Depending upon the wetness condition and other composition of the soil, the permittivity and conductivity can vary in a wide range [6].

In a GPR system, the signals hitting the target and reflecting to the antenna undergoes a frequency dependent attenuation owing to the electrical conductivity of the medium. This is in addition to the loss, which is proportional to the square of the distance. The reflected amplitude is further determined by the electric permittivity of the medium and the target. The reflected amplitude is too small if the permittivity contrast of target and the medium is small. A deep probing requires a low frequency signal, that penetrates without much attenuation. For high-resolution imaging, a large bandwidth is required. Obtaining ultra-wide bandwidth at sub-gigahertz frequencies is a challenging task for GPR antenna designers. High frequency signals are highly attenuated as skin depth is inversely proportional to the square root of frequency. So, most GPRs are designed for sub-gigahertz frequencies. But, the bandwidth has to be large enough to get a high-resolution image of the target. A moderate gain is also desired to meet the link budget requirements. Size of the antenna is also an important factor as the GPR system has to be portable.

Bowtie antennas are most widely used in GPR due to wide impedance matching and radiation properties [1]. These antennas are mostly useful only in a 4:1 bandwidth. Beyond that, there is a reduction in boresight gain. Many GPR systems use resistive loaded bowtie antennas to reduce the size and for increased bandwidth, thus sacrificing the gain and efficiency. This is a major drawback. Bowtie antennas can be loaded with lumped resistors to attenuate the current at the antenna end to suppress the reflections. This will result in a large bandwidth and good pulse radiating ability. Another approach is to provide a continuous loading profile that increases towards the antenna end, which is found to be very good for pulse radiation. Many designs of resistive loaded bowtie antennas are available in the literature [7]–[9].

In this paper, we examine the detection capabilities of RC loaded bowtie and a novel loop loaded bowtie in an experimental GPR setup. RC loaded bowtie antenna having

a 10:1 bandwidth (0.3–3 GHz) had been designed by the authors [10]. The loop-loaded bowtie antennas has been recently designed by the authors [11]. The antenna has a 11:1 impedance bandwidth (0.5–5.5 GHz) without applying any kind of resistive loading. It has a very good gain and efficiency in the entire band. A stable radiation pattern has been obtained throughout the band. The measured results are interesting. Loading the bowtie antenna with a loop is an excellent way to confine the near field of the emitter.

A brief description of the considered antennas is given in Section 2. Simulated and measured parameters are presented and discussed in Section 3. Experimental results of GPR survey are given in Section 4. Section 5 concludes the work.

2. Description of the Antennas

Two types of antennas are considered and compared in this paper. The first is a RC loaded bowtie and the second one is a loop loaded bowtie. The design and optimization of these antennas were carried out by using a commercial electromagnetic simulation software CST Microwave Studio.

2.1. RC Loaded Bowtie Antenna

The RC loaded bowtie antenna is designed for the 300 MHz – 3 GHz frequency range, as described in [10]. It is constituted by two half-ellipses. Periodic slots are cut on the antenna arms, which act as capacitive loading. A graphite sheet of 1 mm thickness is placed over each arm to provide a resistive loading. The combined resistive-capacitive loading enhances the bandwidth while maintaining the compact size 30×23 cm. The antenna is fed using a vertical microstrip to parallel stripline transition. The dimensions with reference to Fig. 1 are: $W = 220$ mm, $L = 286$ mm, $g = 1.5$ mm on FR4 substrate (relative permittivity 4.4) of dimensions 300×230 mm and thickness 1.5 mm (Fig. 3a).

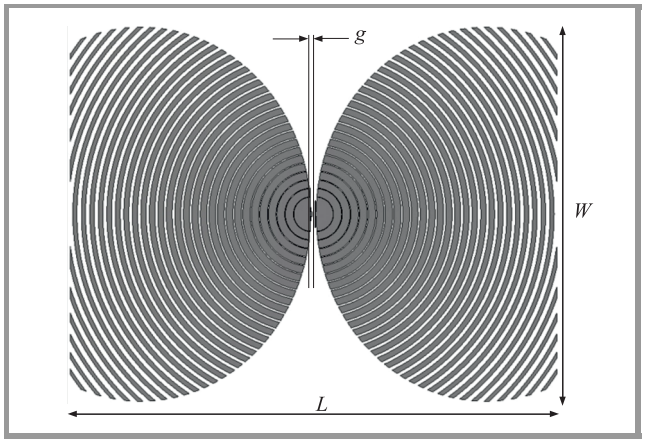

Fig. 1. Geometry of RC bowtie antenna.

2.2. Loop Loaded Bowtie Antenna

The geometry of the loop loaded bowtie antenna is depicted in Fig. 2. This antenna does not require any kind of dissipative loading. Each bowtie arm is etched on either side of the substrate. One of the arm is fed with a simple microstrip feed, while the other arm on the opposite side acts as ground plane. The overall size of the antenna is 23×23 cm. The dimensions with reference to Fig. 2 are: $W = 230$ mm, $L_b = 172$ mm, $R = 196$ mm, $g = 1.5$ mm. FR4 glass epoxy substrate (relative permittivity 4.4) with thickness 1.6 mm has been chosen for the design (Fig. 3b).

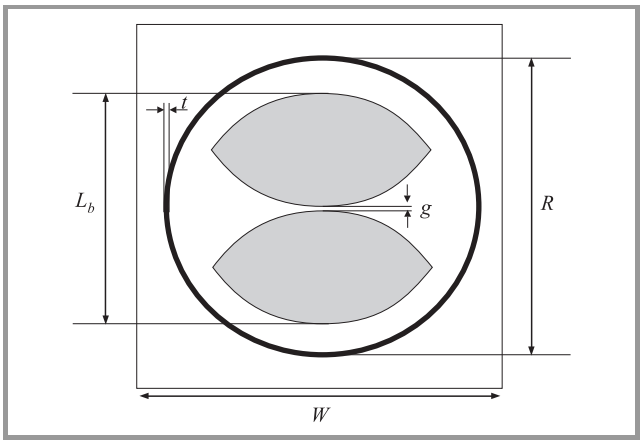

Fig. 2. Geometry of loop bowtie antenna.

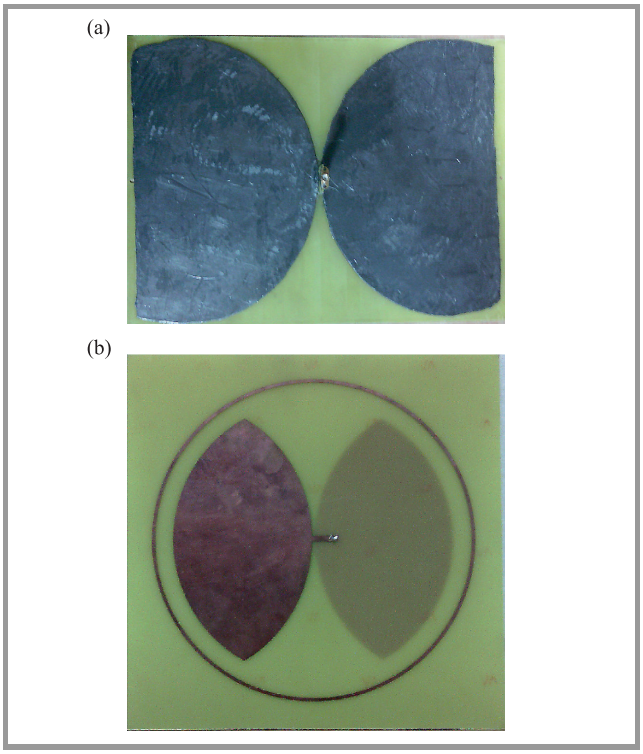

Fig. 3. RC bowtie antenna (a) and loop bowtie antenna (b).

3. Simulation and Measurement of Antenna Parameters

Simulations were carried out by using the time-domain solver, based on the Finite Integration Technique (FIT), implemented in CST Microwave Studio. The meshing parameters were properly chosen, to represent correctly the smallest features of the antenna geometry. In particular, we applied the following rules of thumb: the largest mesh cells must be at least $\frac{\lambda}{10}$ at the highest frequency of simulation. The lower mesh limit must be appropriate for the modeling of the smallest dimensions of the geometry. The vacuum bounding box surrounding the antenna must be at a distance of $\frac{\lambda}{4}$ at the lowest frequency of interest.

3.1. Bandwidth

Figure 4 shows the simulated and measured magnitude of the S_{11} parameter for the RC bowtie. The graph indicates a 10 dB return loss in the frequency range 0.3–3 GHz, for a good impedance match with a 50 Ω feed. The bandwidth is 2.7 GHz. Figure 5 shows the magnitude of the S_{11} parameter for the loop bowtie. The impedance bandwidth, as can be observed from the figure, is centered on 3 GHz and in the 0.5–5.5 GHz interval. This corresponds to a 11:1 bandwidth.

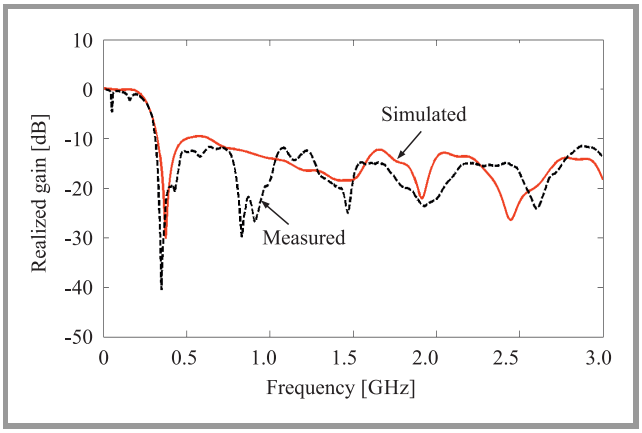

Fig. 4. Measured $|S_{11}|$ vs. frequency of RC bowtie.

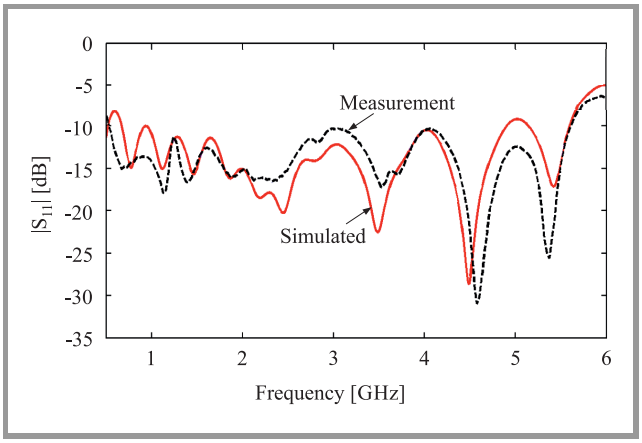

Fig. 5. Measured $|S_{11}|$ vs. frequency of loop bowtie.

3.2. Realized Gain

The realized gain was measured by exploiting a method based on Friis transmission formula and by using two identical antennas as outlined in [12]. The measured gain of the two antennas is plotted in Fig. 6. The gain of the RC loaded bowtie decreases considerably after 1.25 GHz. This is a drawback of the bowtie antenna – the forward gain drastically reduces after a two-octave bandwidth. The loop bowtie has a positive gain in the entire bandwidth, around an average value of 3.13 dBi. The reflected fields from the ring around the bowtie reach the center with the same phase and this significantly improves the forward gain throughout the operating frequency band. The peak gain is also higher compared to the RC bowtie.

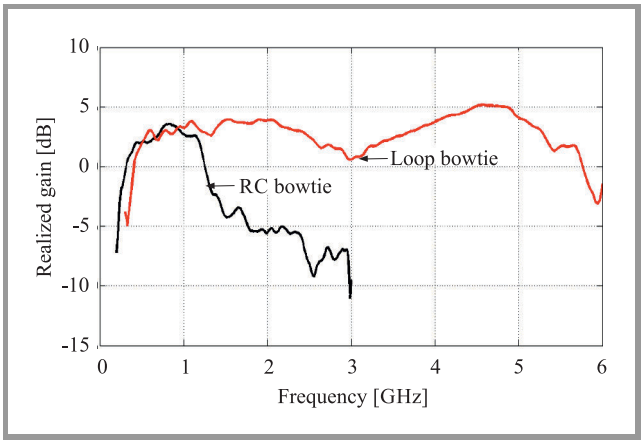

Fig. 6. Realized gain vs. frequency.

The characteristics of the two antennas are summarized in Table 1.

Table 1
Summary of antenna characteristics

Antenna type	Bandwidth	Peak gain	Average gain
RC loaded bowtie	0.3–3 GHz	3.6 dBi	–2.8 dBi
Loop bowtie	0.5–5.5 GHz	5.2 dBi	3.13 dBi

3.3. Radiation Pattern

Radiation pattern measurements were carried out in outdoor environment. The measured radiation patterns of the RC bowtie antenna, in the E and H planes, at two representative frequencies (1 and 2.5 GHz) are shown in Fig. 7. The pattern is close to a "figure of 8" in the E-plane and omni-directional in the H-plane, at lower frequencies. One can observe the sharp null in the boresight at 2.5 GHz. The measured radiation patterns of the loop bowtie at the designated frequencies are presented in Fig. 8. Boresight radiation has been significantly improved at 2.5 GHz, due to the loop.

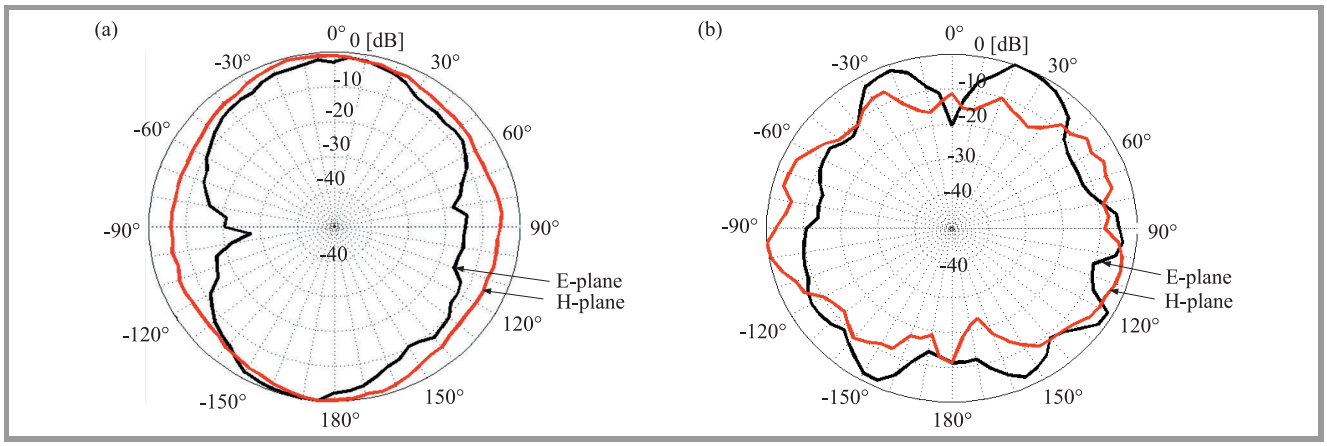

Fig. 7. E-plane and H-plane radiation pattern of RC bowtie at: (a) 1 GHz and (b) 2.5 GHz.

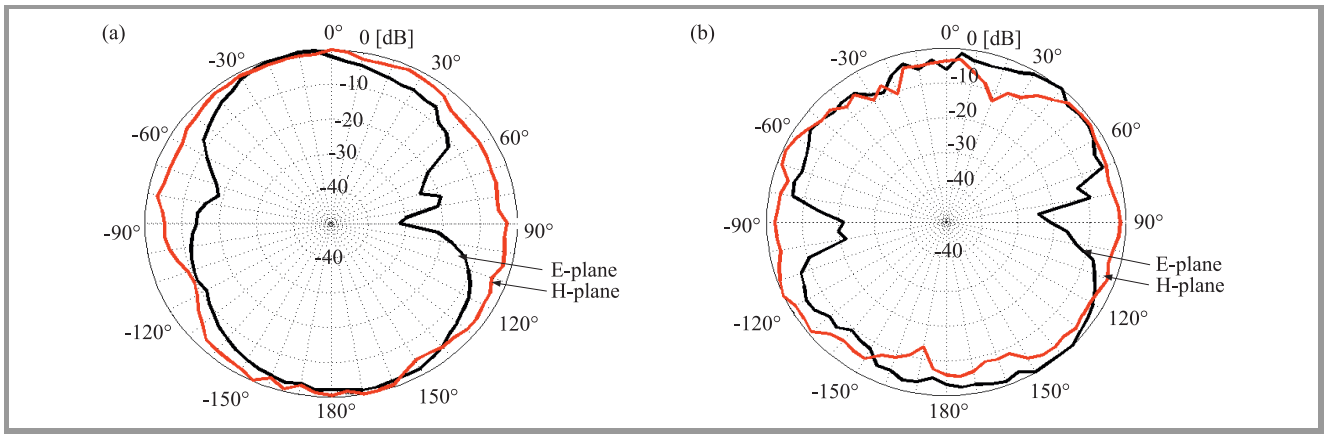

Fig. 8. E-plane and H-plane radiation pattern of loop bowtie at: (a) 1 GHz and (b) 2.5 GHz.

4. Results of GPR Experiments

Our experimental GPR comprises a portable Vector Network Analyzer (VNA) and a single antenna for transmission and reception of signals. The antenna is used without any reflector. The photograph of the setup is shown in Fig. 9. The transmitting/receiving antenna is connected to port 1 of the VNA. The frequency is swept from 300 MHz to 3 GHz, in steps of 4.5 MHz. Complex reflection coefficient data are acquired at a spatial interval of 2 cm, along a horizontal line. Each instance of measurement is called one A-scan. Inverse Fourier transform of the collected frequency domain data gives the time domain data. Ensemble of A-scans along a line gives the B-scan image of the target. The clutter in the image is removed by a simple averaging procedure, as outlined in [13].

To compare the performance of the antennas, GPR surveys were carried out to detect four types of targets:

1. a brass pipe of diameter 2.54 cm,
2. a galvanized iron pipe of diameter 5.08 cm,
3. a dry bamboo of diameter 7 cm and,
4. reinforcement bars inside concrete.

The depth of the target is about 40 cm from the antenna in the first three cases. In the fourth experiment, the depth of

Fig. 9. Photograph of the experimental GPR.

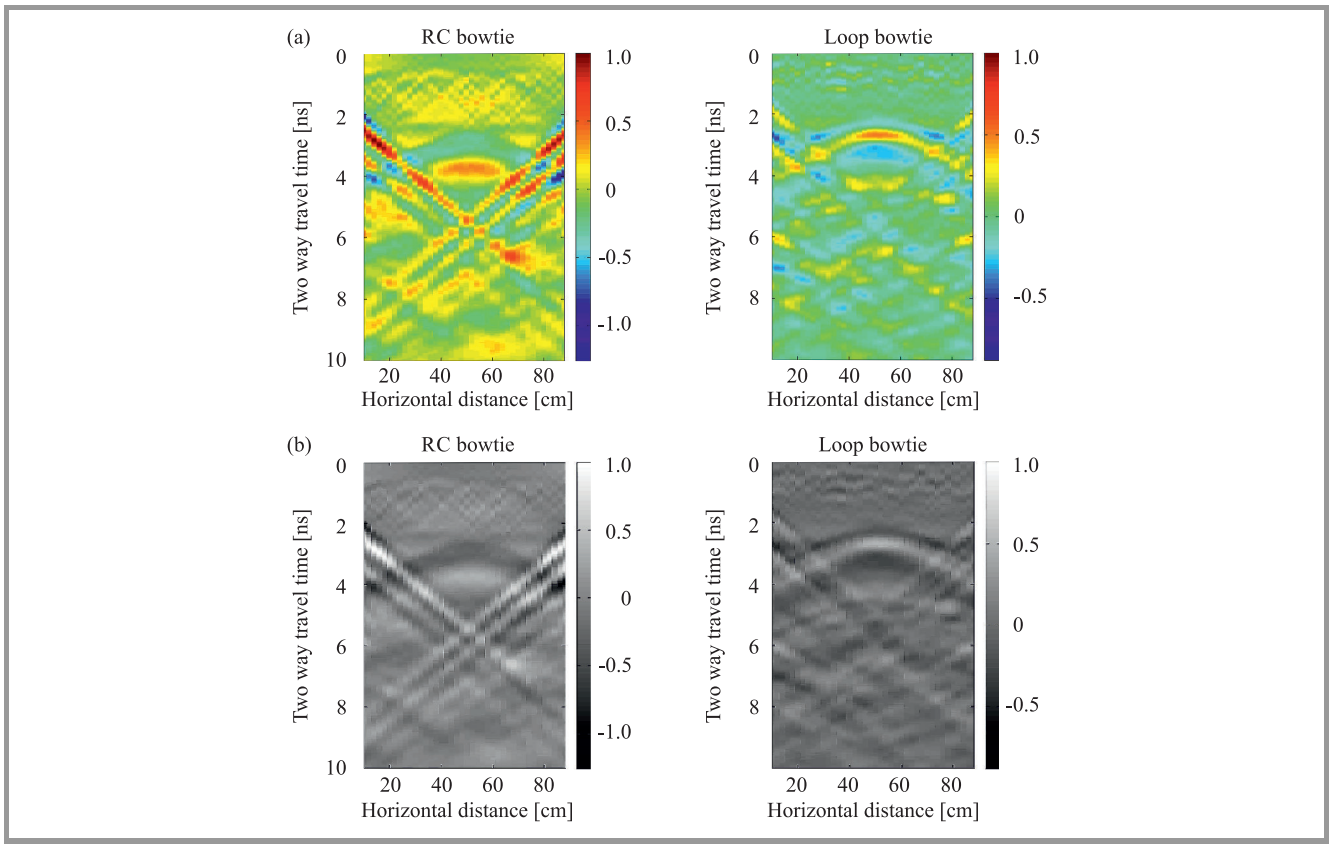

Fig. 10. Color (a) and gray scale GPR images of brass pipe (b). (See color pictures online at www.nit.eu/publications/journal-jtit)

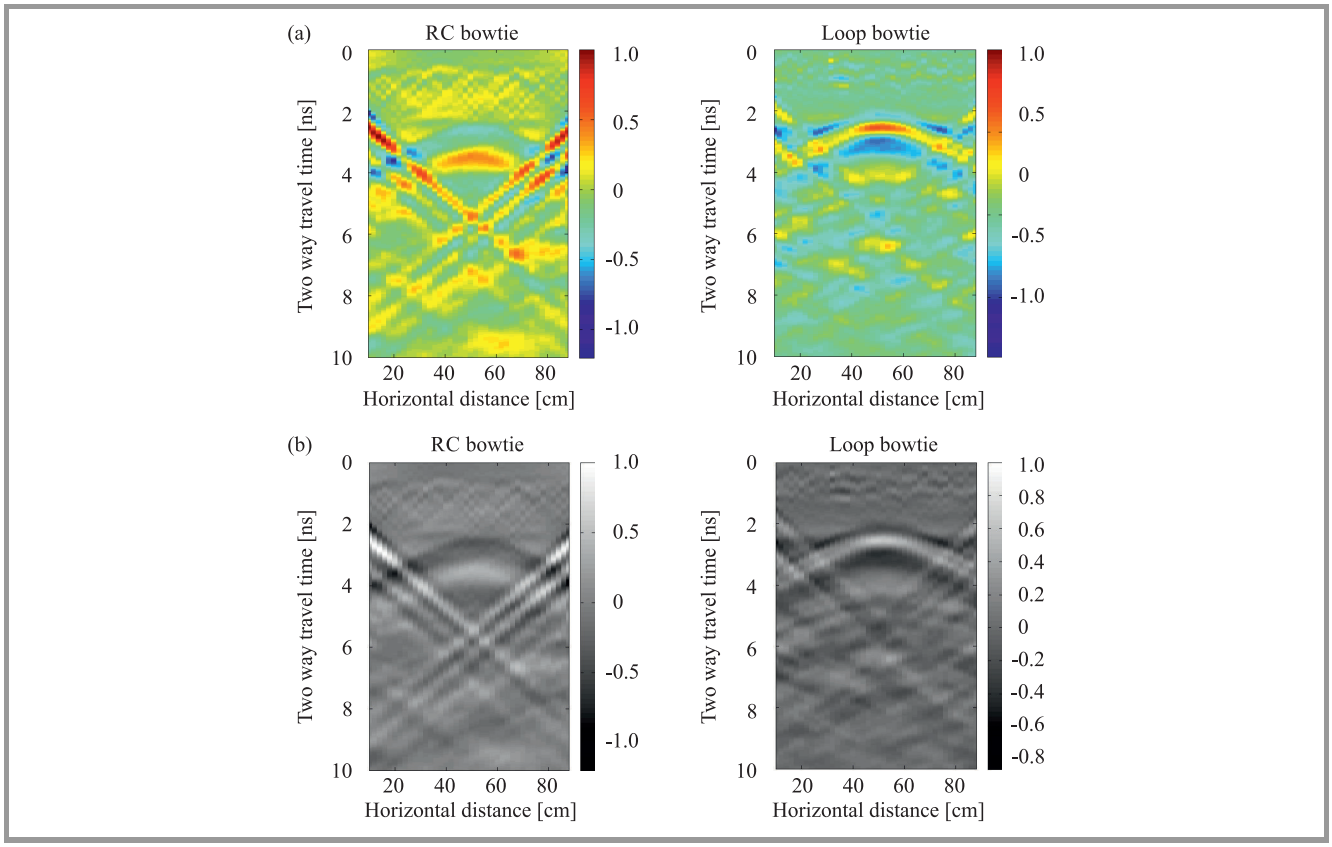

Fig. 11. Color (a) and gray scale GPR images of galvanized iron pipe (b).

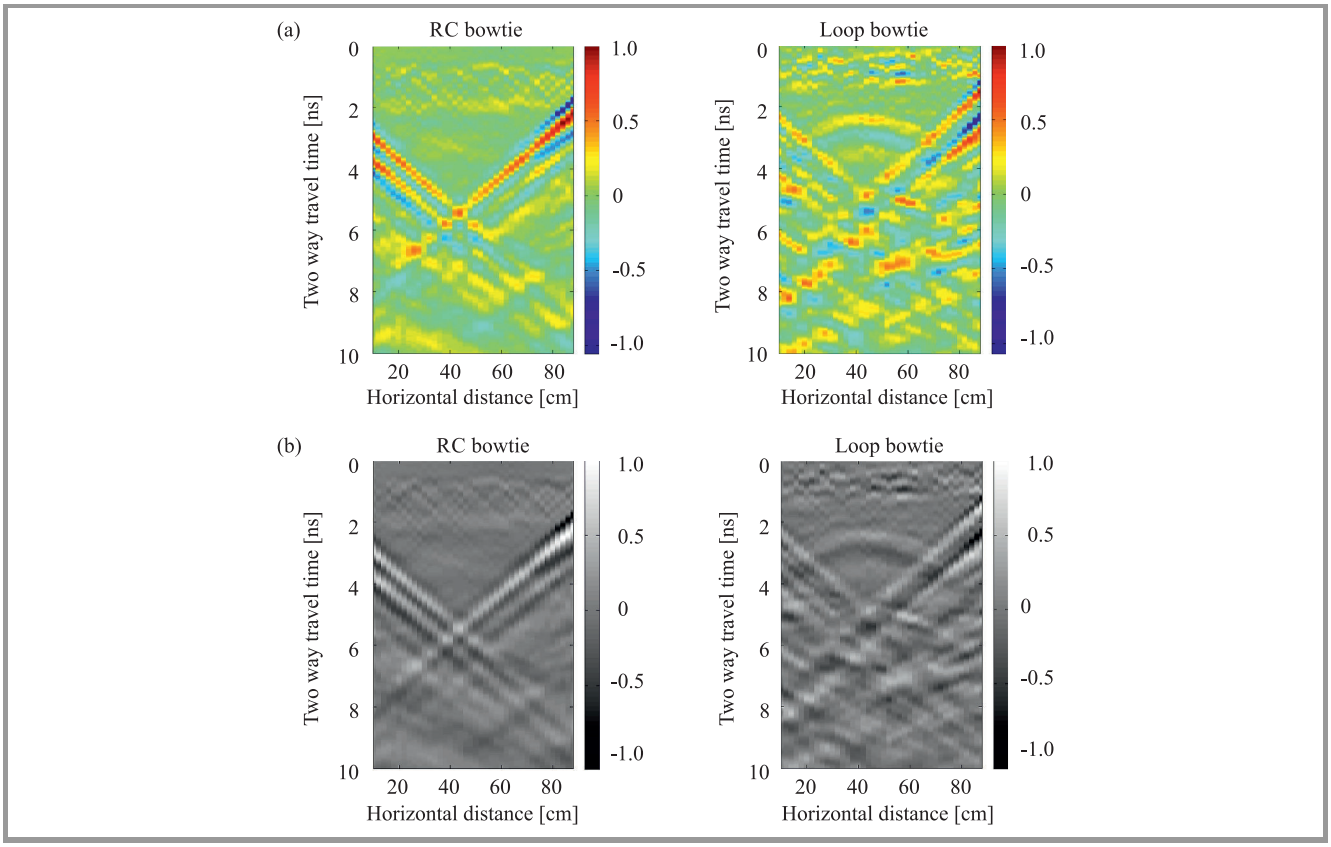

Fig. 12. Color (a) and gray scale GPR images of dry bamboo (b).

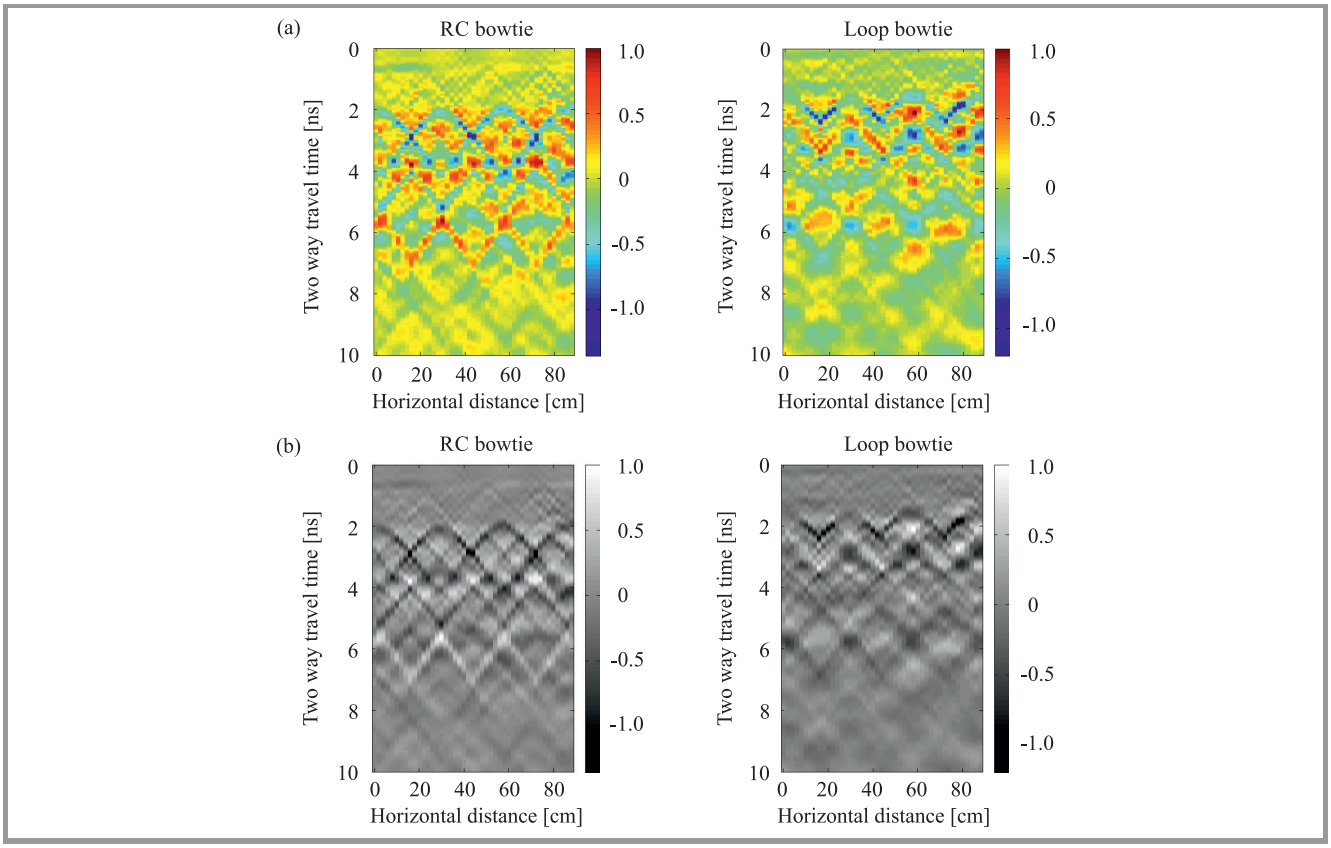

Fig. 13. Color (a) and gray scale GPR images of reinforcement bars in concrete (b).

the rebar and the distance between the bars are not known to us. Due to the fact that the bowtie antenna is linearly polarized, the antenna axis is aligned with the target to maximize the return signal.

Let us start with results obtained in the first experiment, i.e. when the target was a brass pipe. Figure 10 shows the GPR images in color and gray scale. The target is located at the apex of the hyperbola, about 50 cm on the horizontal axis. It can be seen that the image produced by the loop bowtie is sharper and more clutter free, compared to that produced by the RC bowtie.

In the second experiment, the target was a galvanized iron pipe of diameter 5.08 cm. Figure 11 shows the detected image of the pipe. In this case, too, a better image is obtained with the loop bowtie compared to the RC bowtie.

In the third experiment, the target was a dry bamboo. The GPR images are shown in Fig. 12. In the previous cases, the targets were metallic, hence reflections from the targets were high. But, in this case, there is a dielectric target and the dielectric contrast between the target and the surrounding medium is smaller. So, the reflections from the target are rather weak. From the figure, it is observed that RC bowtie could not produce an image of the target. Even in this case, the image produced by loop bowtie has been exemplary. So, a potential application of the loop bowtie antenna may be in detection of non-metallic landmines.

In the fourth experiment, a GPR survey of concrete roof was conducted in order to detect the rebar inside. The image obtained is shown in Fig. 13. The reinforcement bars separated by a distance of about 25 cm are visible in the image. In the case of the RC bowtie, there are multiple hyperbolas below the actual location of rebar. With the loop bowtie, those clutters are not much visible in the image.

5. Conclusion

The performance of two types of antennas for GPR: a RC loaded bowtie and a novel loop bowtie, has been experimentally studied and compared. GPR images produced by the loop loaded antenna turned out to be better than those produced by the RC loaded bowtie, for all the test targets considered. The loop loading technique can be employed in existing antennas also, to enhance the radiation properties. The results presented in this paper emphasize the role of efficient antennas for improved GPR detection capability. This also signifies the importance of more research required to design efficient ultra-wideband antennas at sub-gigaherz frequencies, for GPR and similar applications.

Acknowledgements

We thank the Guest Editors Lara Pajewski, Hovik Baghdasaryan and Marian Marciniak for inviting us to participate in the JTIT Special Issue “Recent Progress in Electromagnetic Theory and its Applications”, organized by the COST Action TU1208 “Civil engineering applications of Ground Penetrating Radar”.

References

[1] A. Benedetto and L. Pajewski, Eds., *Civil Engineering Applications of Ground Penetrating Radar*. Book Series: “Springer Transactions in Civil and Environmental Engineering”. Springer International Publishing Switzerland, 2015.

[2] C. W. Chang, C. H. Lin, and H. S. Lien, “Measurement radius of reinforcing steel bar in concrete using digital image GPR”, *Constr. and Build. Mater.*, vol. 23, no. 2, pp. 1057–1063, 2009.

[3] S. Hong, W. W.-L. Lai, G. Wilsch, R. Helmerich, R. Helmerich, T. Günther, and H. Wiggenhauser, “Periodic mapping of reinforcement corrosion in intrusive chloride contaminated concrete with GPR”, *Constr. and Build. Mater.*, vol. 66, pp. 671–684, 2014.

[4] C. J. Vaughan, “Ground Penetrating Radar surveys used in archaeological investigations”, *Geophys.*, vol. 51, no. 3, pp. 595–604, 1986.

[5] T. Montoya and G. Smith, “Land mine detection using a groundpenetrating radar based on resistively loaded Vee dipoles”, *IEEE Trans. on Antenn. and Propag.*, vol. 47, no. 12, pp. 1795–1806, 1999.

[6] H. M. Jol, *Ground Penetrating Radar Theory and Applications*. Elsevier Science, 2008.

[7] A. Lestari, A. Yarovoy, and L. Ligthart, “RC-loaded bow-tie antenna for improved pulse radiation”, *IEEE Trans. on Antenn. and Propag.*, vol. 52, no. 10, pp. 2555–2563, 2004.

[8] A. A. Lestari, A. G. Yarovoy, and L. P. Ligthart, “Adaptive wire bow-tie antenna for GPR applications”, *IEEE Trans. on Antenn. and Propag.*, vol. 53, no. 5, pp. 1745–1754, 2005.

[9] A. A. Lestari, E. Bharata, A. B. Suksmono, A. Kurniawan, A. G. Yarovoy, and L. P. Ligthart, “A modified bow-tie antenna for improved pulse radiation”, *IEEE Trans. on Antenn. and Propag.*, vol. 58, no. 7, pp. 2184–2192, 2010.

[10] K. K. Ajith and A. Bhattacharya, “Printed compact lens antenna for UHF band applications”, *Progress in Electromag. Res. C*, vol. 62, pp. 11–22, 2016.

[11] K. K. Ajith and A. Bhattacharya, “Improving the detectability and imaging capability of ground penetrating radar using novel antenna concepts”, in *EGU General Assembly Conference Abstracts*, ser. EGU General Assembly Conference Abstracts, vol. 19, Apr. 2017, p. 7562.

[12] C. A. Balanis, *Antenna Theory: Analysis and Design*. Hoboken, NJ: Wiley, 2005.

[13] D. J. Daniels, Ed., *Ground Penetrating Radar*. The Institution of Engineering and Technology, Michael Faraday House, Six HillsWay, Stevenage SG1 2AY, UK: IET, Jan 2004.

K. K. Ajith received his B.Tech. degree from Kannur University and M.Tech. degree from Cochin University of Science and Technology in 2006 and 2009 respectively. He worked as Assistant Engineer (Electrical) at Kerala State Electricity Board from Nov. 2009 to Dec 2011. Since 2011, he is pursuing Ph.D. at Indian Institute of Technology Kharagpur. He is working as an Assistant Professor at department of ETC, IIIT Bhubaneswar since Dec. 2016. His areas of interests are: printed antennas, metamaterials and GPR.

E-mail: ajithkkoroth@gmail.com
Department of ETC
International Institute of Information Technology
Bhubaneswar
751003, India

Amitabha Bhattacharya received the B.Tech., M.E. and Ph.D. degrees in Electronics and Electrical Communication Engineering from I.I.T. Kharagpur, Jadavpur University, Calcutta, and I.I.T. Kharagpur, in- 1986, 1994, and 1998, respec–tively. Since July 2007, he has been with the I.I.T Kharagpur, where he is now an Associate Professor of Electronics and Electrical Communication Engineering. His present research interest is in the field of microwave imaging, GPR systems analysis and EM propagation.

E-mail: amitabha@ece.iitkgp.ernet.in
Department of E & ECE
Indian Institute of Technology Kharagpur
721302, India